

Energy

Elsevier Editorial System(tm) for Solar

Manuscript Draft

Manuscript Number:

Title: First examples of pyran based colorants as sensitizing agents of p-type dye-sensitized solar cells

Article Type: Research paper

Section/Category: Photovoltaic materials and systems

Keywords: NiO; Dye-Sensitized Solar Cells; Pyran-based dyes; NIR-Dyes

Corresponding Author: Dr. Matteo Bonomo,

Corresponding Author's Institution: La Sapienza

First Author: Matteo Bonomo

Order of Authors: Matteo Bonomo; Roberto Centore; Aldo Di Carlo; Antonio Carella; Danilo Dini

Abstract: Three different pyran based dyes were synthesized and tested for the first time as photosensitizers of NiO based p-type dye-sensitized solar cells (p-DSSC). The molecules feature a similar molecular structure and are based on a pyran core that is functionalized with electron acceptor groups of different strength and is symmetrically coupled to phenothiazine donor branches. Optical properties of the dyes are deeply influenced by the nature of the electron-acceptor group, so that the overall absorption of the three dyes covers the most of the visible spectrum. The properties of devices based on the NiO electrodes sensitized with the investigated dyes were evaluated under simulated solar radiation: the larger short circuit current density exceeded 1 mA/cm² and power conversion efficiency as high as 0.04 % could be recorded. The performances of the fabricated p-DSSC have been compared to a reference cell sensitized with P1, a high level benchmark, which afforded a photoelectrochemical activity similar to the best example of our pyran sensitized devices (1.19 mA/cm² and 0.049 %).

Suggested Reviewers: Claudia Barolo

Claudia.barolo@unito.it

Her wide experience in DSSC (especially in the synthesis of NIR dyes)

Mirko Congiu

mirko.congiu@fc.unesp.br

His wide experience in semiconducting material for PV application.

Alessandro Latini

alessandro.latini@uniroma1.it

His experience in DSSC.



Università degli Studi "La Sapienza" di Roma

DIPARTIMENTO DI CHIMICA

Prof. Danilo Dini

Tel.: -39-06-4991 3335

Fax: -39-06-490324

e-mail: danilo.dini@uniroma1.it

Rome , 12th May 2017

Dear Editor,

the manuscript we intend to submit for consideration of publication in *Solar Energy* reports for the first time the photoelectrochemical properties of p-type dye-sensitized solar cells (p-DSCs), which employ nanostructured NiO photocathodes previously sensitized by pyran based colorants. The series of dye-sensitizers here proposed represents an original choice in the framework of the research on p-DSCs. The light conversion performance of the photoelectrochemical cells here described for the first time compares to the ones of the best performing devices of the same type. For these reasons we believe that the content of the present work fits with the aims of this journal and attracts the interest of a broad audience ranging from organic chemists to electrochemists and materials scientists that are involved in the science of p-DSCs and analogous solar conversion devices.

Thank you for the consideration.

Best regards,

Danilo Dini

A handwritten signature in black ink, appearing to read 'Danilo Dini', written in a cursive style.

1 First examples of pyran based colorants as sensitizing agents of *p*-type dye- 2 sensitized solar cells 3

4
5
6 3 Matteo Bonomo,^a Roberto Centore,^b Aldo Di Carlo,^c Antonio Carella,^{b*} Danilo Dini^{a*}
7

8
9
10 4 a: Dept. of Chemistry, University of Rome “La Sapienza”, p.le Aldo Moro 5, 00185 Rome (Italy)
11

12 6 b: Dept. of Chemical Sciences, University of Naples Federico II, Complesso Universitario Monte
13 7 Sant’Angelo, via Cintia, 80126 Naples (Italy)
14

15 8
16 9 c: Centre for Hybrid and Organic Solar Energy (CHOSE), Dept. of Electronic Engineering,
17 10 University of Rome “Tor Vergata”, via del Politecnico 1, 00133 Rome (Italy)
18

19 11
20
21 12 *to whom correspondence should be addressed. e-mail antonio.carella@unina.it and
22 13 daniilo.dini@uniroma1.it
23

24 25 14 26 15 **Abstract**

27
28
29
30 16 Three different pyran based dyes were synthesized and tested for the first time as photosensitizers
31
32 17 of NiO based *p*-type dye-sensitized solar cells (*p*-DSSC). The molecules feature a similar molecular
33
34 18 structure and are based on a pyran core that is functionalized with electron acceptor groups of
35
36 19 different strength and is symmetrically coupled to phenothiazine donor branches. Optical properties
37
38 20 of the dyes are deeply influenced by the nature of the electron-acceptor group, so that the overall
39
40 21 absorption of the three dyes covers the most of the visible spectrum. The properties of devices
41
42 22 based on the NiO electrodes sensitized with the investigated dyes were evaluated under simulated
43
44 23 solar radiation: the larger short circuit current density exceeded 1 mA/cm² and power conversion
45
46 24 efficiency as high as 0.04 % could be recorded. The performances of the fabricated *p*-DSSC have
47
48 25 been compared to a reference cell sensitized with **P1**, a high level benchmark, which afforded a
49
50 26 photoelectrochemical activity similar to the best example of our pyran sensitized devices (1.19
51
52 27 mA/cm² and 0.049 %).
53
54
55
56
57
58
59
60 28
61
62
63
64
65

29 INTRODUCTION

1
2
3
4
5
6
7
8
9
10
11
12
13
14
15
16
17
18
19
20
21
22
23
24
25
26
27
28
29
30
31
32
33
34
35
36
37
38
39
40
41
42
43
44
45
46
47
48
49
50
51
52
53
54
55
56
57
58
59
60
61
62
63
64
65

Dye-sensitized solar cells (DSSCs) represent one of the emerging photovoltaic technology which gained a considerable interest in the last twenty years[1–8] as a viable low cost alternative to traditional photovoltaics based on silicon modules[9]. DSSCs technology presents further appealing features as optical transparency, the possibility of being realized in different colours and the possibility to be integrated in architectural elements different from the roof, so paving the way to the so-called building integrated photovoltaics[10,11]. The heart of a DSSC device is a wide bandgap semiconductor oxide, sensitized with a photoactive dye able to inject, upon photoexcitation, electrons (*n*-type) or holes (*p*-type) in the semiconductor substrate. Following the seminal work of Grätzel and O’Regan[12], *n*-type DSSC have been thoroughly investigated and a power conversion efficiency (PCE, η) exceeding 14 % have been reached[13]. Conversely, the number of studies regarding *p*-type DSSCs is significantly lower[14–19] but it is increasing in the last years as it has become clear that efficiency of *n*-type DSSC has reached a plateau: these kinds of devices are in fact extremely interesting because they open the way to the realization of tandem DSSC device[20,21] based on the connection of a *p*-type photoelectrode with a *n*-type photoelectrode, each contributing to the total photovoltage generated by the cell. Applying this concept, photovoltaic devices with a theoretical efficiency up to 40 % could be obtained[22,23]. However, so far, the performances of *p*-DSSCs[24] remain a way lower than the *n*-type counterparts, with a maximum reported PCE of 2.5 %[25]. Different reasons can explain the poor performance of these devices: the typically used photocathode, NiO, suffer from some intrinsic drawbacks, as low hole mobility[26], which is consequential to a stronger bond between the injected hole and electron residing on the dye, thus easing the detrimental charge recombination process, and low dielectric constants[19]. The latter feature lowers the radiation penetration depth (self absorption phenomenon). Moreover, the valence band position of NiO, relatively to the classically used iodide/triiodide redox mediator, limits the maximum attainable V_{oc} [27].

55 Optimization of both *p*-type semiconductor and electrolyte is undoubtedly required for improving
1
256 the performance of *p*-DSSC. The sensitizers as well play a very important role[28–32]: absorption
3
4
57 in a broad range of the solar spectrum along with high molar extinction coefficients are highly
6
758 desirable. Moreover, it is essential that, upon photoexcitation, electron density moves away from
8
9
59 the anchoring points on NiO surface so that charge recombination occurs at lower rate. The design
10
11
1260 of novel dyes that fulfil such requirements is then highly demanded in the way for high efficiency
13
14
1561 *p*-DSSC devices. Pyran based dyes are molecular systems that have shown interesting properties for
16
1762 applications in different field of organic electronics e.g. as red emitters in OLED[33,34] or
18
19
2063 photovoltaic materials[35,36], and photonics, for their nonlinear optical properties[37–42]. Their
21
2264 synthetic procedure is well established and affords a chemical structure typically based on a pyran
23
2465 core functionalized with an electron acceptor group and symmetrically linked to donor conjugated
25
26
2766 branches; this kind of structure could be extremely interesting for the application of these molecular
28
2967 systems as photosensitizers in *p*-DSSCs because it is in principle possible design chromophores
30
31
3268 with an electron acceptor core placed far away from peripheral groups acting as anchoring units for
33
3469 binding the dye to NiO surface. Their use in *p*-DSSC is, up to our knowledge, not yet reported
35
36
3770 while in the literature some examples of their application as photosensitizers in *n*-type DSSCs can
38
3971 be found[43–45]. In particular, in a recent work[45], some of us prepared the dyes reported in
40
4172 Figure 1 and used them as photosensitizers for classical Grätzel cells.

42
43
4473 The functionalization of the same molecular core (pyran) with electron acceptor groups of
45
4674 increasing strength (moving from dyes **CB1** to **CB3**) resulted in the tuning of the optical absorption
47
48
4975 properties of the dyes and in the obtainment of chromophores the colour of which ranged from
50
5176 orange to blue, so covering most part of the visible spectrum. A moderate efficiency, up to 2.8 %,
52
53
5477 was reported in this paper[45]. One of the factors limiting the efficiency of these photosensitizers in
55
5678 *n*-DSSC is that, upon photoexcitation, electron density moves away from the peripheral carboxylic
57
5879 groups (representing the anchoring points of the dyes on TiO₂ surface). This feature hinders the
59
60
61
62
63
64
65

80 electron injection process from the dye to the semiconductor oxide thus limiting the overall
1 efficiency.
2
3
4
5

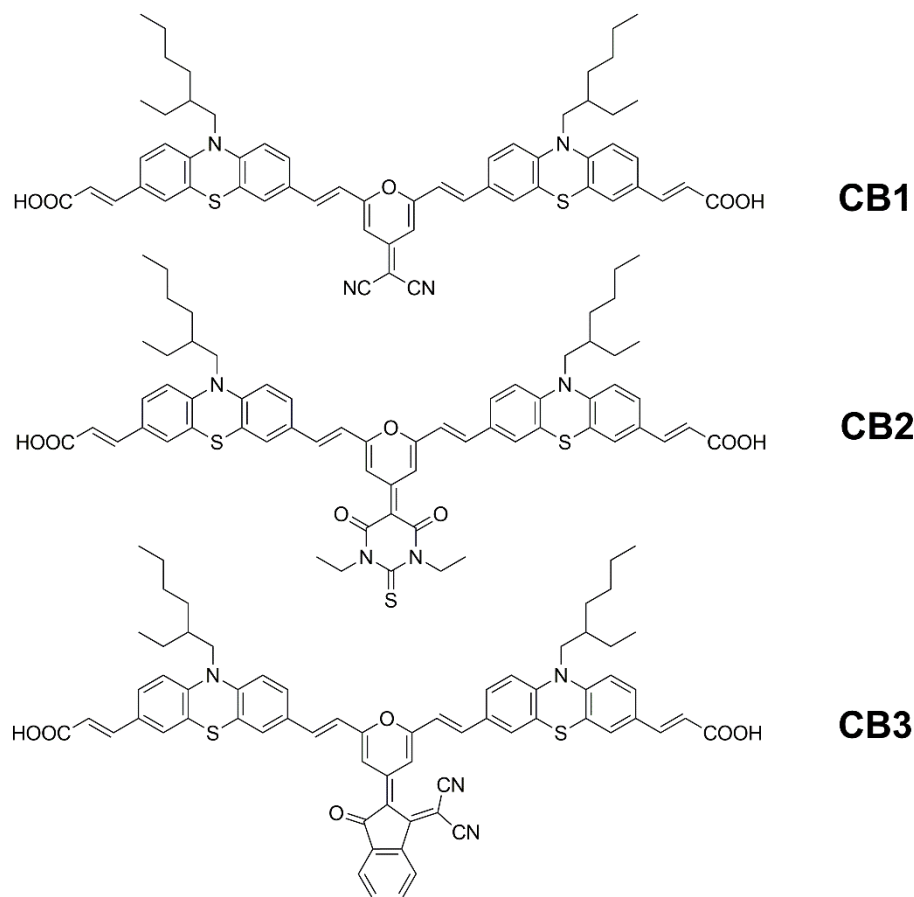


Figure 1. Chemical structures of the reported pyran based photosensitizers

43 At the same time, as previously mentioned, this behaviour is highly desirable if the dyes must be
44 used as photosensitizers for *p*-DSSC[46]. This consideration prompted us to explore the potentiality
45 of these molecular systems in the field of *p*-DSSC: the devices have been prepared by sensitizing
46 of these molecular systems in the field of *p*-DSSC: the devices have been prepared by sensitizing
47 NiO thin film and using iodide/triiodide as redox mediator[47].The fabricated devices have been
48 photoelectrochemically characterized under simulated solar radiation and the contribution to current
49 generation by each single wavelength was determined by the analysis of the IPCE (incident photon-
50 to-current conversion efficiency) spectra.
51
52
53
54
55
56
57
58
59
60
61
62
63
64
65

93 **EXPERIMENTAL**

94
95 The details regarding the synthesis of the dyes as well as their optical, electrochemical and the
96 computed electronic properties, have been previously reported elsewhere[44,45]. For what concerns
97 the preparation of the photocathode, we adopted a procedure described in previous works from
98 us[46,48]. As far as the preparation of screen-printed NiO electrodes is concerned, preformed NiO
99 nanospheres (with a diameter smaller than 50 nm) have been grinded in a mortar and hydrochloric
100 acid (1 mL), H₂O (5 mL), ethanol (30 mL), terpineol (20 mL) and ethylcellulose (10% w/w in
101 ethanol solution) were added. All chemicals employed were purchased from Sigma-Aldrich or
102 Fluka at the highest degree of purity available and they were used without any further purification.
103 Both addition and grinding of the various mixtures have been performed at room temperature. After
104 the addition of terpineol and ethylcellulose the solution has been homogenized by stirring and
105 ultrasonic treatment. Then the mixture has been heated at 50 °C under continuous stirring till the
106 paste had the appearance of a viscous slurry. Anhydrous terpineol was used as a mixture of
107 enantiomers. The ultrasonic homogenization was performed with a Ti-horn-equipped sonicator
108 (Vibracell 72408 from Bioblock scientific). The resulting paste was spread onto a FTO-covered
109 glass via screen-printing and after a pre-drying period of 15 minutes at 120 °C in oven it was
110 sintered at 450 °C for half an hour (heating ramp of 15 °C/min). The thickness of the resulting
111 electrodes (~ 2 μm) was measured with a Dektat 150® profilometer from Veeco.

112 Sensitization of NiO photocathodes was obtained by electrodes dipping in a 0.2 mM dye-sensitizer
113 solution with THF as solvent. All electrodes were sensitized at room temperature for 16 hours.

114 Pt-counter electrodes were prepared by screen-printing onto FTO-coated glass as reported
115 elsewhere[49].

116 NiO photocathodes and Pt-FTO counter-electrodes were assembled in a sandwich configuration
117 using a Bynel® (a thermoplastic polymeric film) as sealant. Bynel® also acts as a spacer that
118 determines the thickness of the cell. The iodine-based electrolyte solution (HSE from Dyesol) was

119 injected inside the device by vacuum backfilling technique. The hole for injection was finally sealed
1
120 with a commercial glass/glass glue. The photoactive area of the samples was 0.25 cm².

121 The measurements of optical transmittance were made with a double ray spectrometer (model UV-
122 2550 from Shimadzu). Photoelectrochemical performances were evaluated using a solar simulator
123 Solar Test 1200 KHS (class B) at 1000 W/m⁻² with artificial solar spectrum AM 1.5 G. The IPCE
124 curves were recorded using a computer controlled set-up consisting of a Xe lamp (Mod.70612,
125 Newport) coupled to a monochromator (Cornerstone 130 from Newport), and a Keithley 2420 light-
126 source meter.

128 RESULTS AND DISCUSSION

129
130 The chemical physical characterization of the dyes has been previously reported[45]. For sake of
131 clarity, in Table 1 the main optical parameters of wavelength of maximum absorption (λ_{\max}) in THF
132 solution, corresponding molar extinction coefficient (ϵ), and the energies of the frontier's
133 molecular orbitals of the dyes are summarized[45]. The energy levels of the highest-occupied
134 molecular orbital (HOMO), and the lowest unoccupied molecular orbital (LUMO) have been
135 estimated by a combined optical-electrochemical approach.

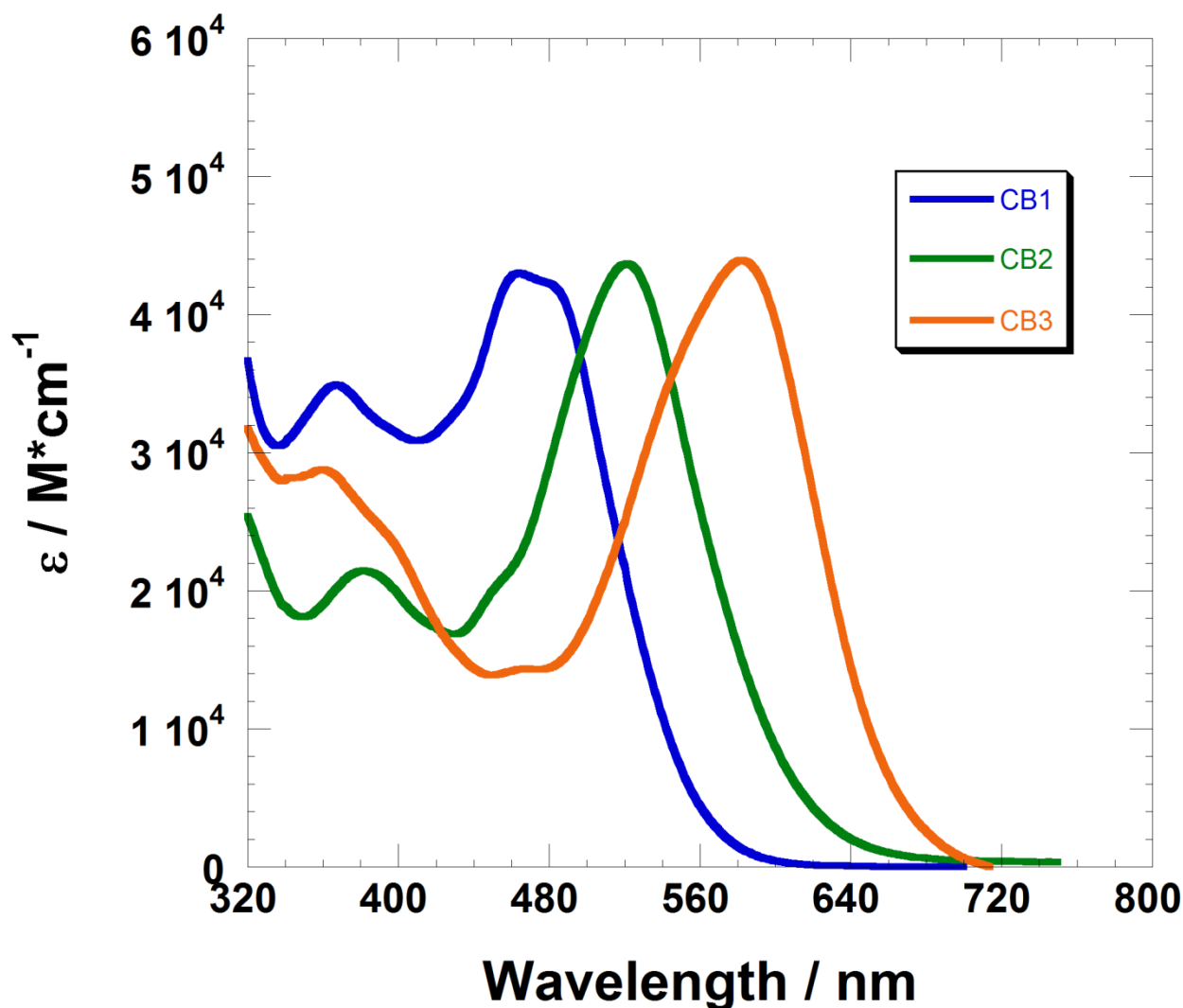
137 **Table 1.** *Optical and electrochemical properties of the synthesized chromophores*

Dye	λ_{\max} /nm ^a	ϵ /L·mol ⁻¹ ·cm ⁻¹ ^a	HOMO /eV ^b	LUMO / eV ^b
CB1	464	4.1·10 ⁴	-5.51	-3.51
CB2	521	4.3·10 ⁴	-5.51	-3.69
CB3	582	3.8·10 ⁴	-5.59	-3.95

138 *a) Scan rate 200 nm/min, in THF solution; b) determined, as reported in ref. 38, by a combined electro-
139 chemical and optical approach on thin film of the dyes.,*

140 The dyes are characterized by a similar chemical structure (see Figure 1) and differ only for the
141 nature of the electron acceptor group which functionalizes the pyran core. The electron-
142 withdrawing strength of this group exerts a strong influence on the optical properties of these dyes

143 as evinced from the data of Table 1 and the absorption spectra of Figure 2. The absorption spectra
1
144 of the dyes in solution were recorded. Upon increasing the strength of the electron withdrawing
2
3
4
145 character of the electron acceptor group that functionalizes the pyran core, the larger is the red shift
5
6
146 of the characteristic absorption of the dye so that the colour of the dye is tuned from orange (dye
7
8
147 **CB1**) to magenta (dye **CB2**) and to blue (dye **CB3**).



47
48
49 **Figure 1.** Molar absorptivity of the reported dyes in THF solution
50

51 The coverage of a such large part of the visible spectrum along with a high molar extinction
52 coefficients presented by all the dyes (up to $4.3 \cdot 10^4$) represent important properties in view of the
53 use of the reported dyes as photosensitizers for DSSC of *p*-type. Energetic levels of the frontier's
54 molecular orbital, estimated by a combined optical-electrochemical approach in the previous paper

155 (see Table 1) are well suited for the application of the dyes in NiO based device (*p*-type DSSCs). In
1 fact, the HOMO energy level of the dyes are placed below the upper edge of NiO valence band
156 (VB) located at -5.0 eV[50,51], while the LUMO energy level of the sensitizer lies above the redox
157 potential of the redox couple I⁻/I₃⁻ (4.8 eV). The latter two features are mandatory to ensure efficient
158 hole injection into the semiconductor VB and regeneration from the redox species. Moreover, the
159 dyes are characterized by the presence of two anchoring groups that allow a firm adhesion of the
160 molecules on an oxide surface as previously shown by the stability measurement of the *n*-DSSC
161 devices with TiO₂ electrodes sensitized with the compounds of Figure 1. A further appealing aspect
162 of the dyes here reported is that the electron withdrawing groups (EWGs) are located far away from
163 the carboxylic anchoring groups. By virtue of this spatial arrangement the EWGs are expected to
164 be oriented far from NiO surface and disfavor kinetically electronic recombination if one assumes
165 that the site of triiodide reduction is mostly localized at the EWG[20,52]. By means of a
166 computational analysis at DFT level it was shown that upon photoexcitation in all the dyes electron
167 density moves from the peripheral part to the core and LUMO of the molecules is localized on the
168 pyran core[45]. This aspect could be of great interest in the application of such dyes as
169 photosensitizers for *p*-DSSC because it results in a minimization of recombination phenomena the
170 LUMO of the dyes being far from NiO surface. At the same time, the localization of the LUMO far
171 from NiO surface can induce the acceleration of the electron transfer (*et*) from the excited dye to the
172 redox shuttle.
173 All these features suggest an efficient use of these dyes in *p*-DSSC. First of all, we tested the
174 goodness of sensitizers chemisorption onto NiO surface. NiO was sensitized as described in
175 Experimental Section. In Figure 3 the transmittance spectra of the sensitized photocathodes are
176 reported: the sensitization provokes a depletion of electrodes transmittance in the absorption region
177 typical of the dyes, as compared to bare NiO. This evidence is a key proof of a good sensitization:
178 all the tested dyes experimented a very good binding.

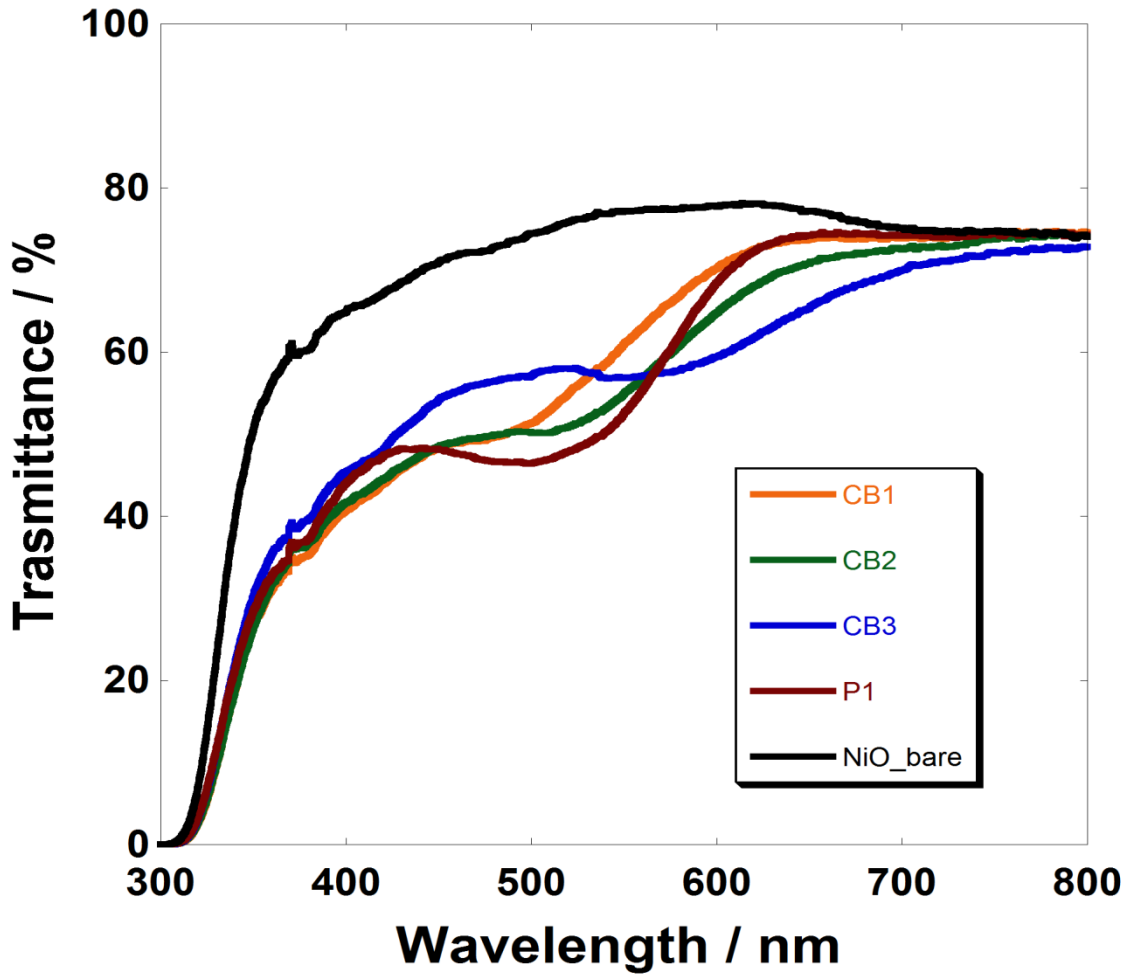
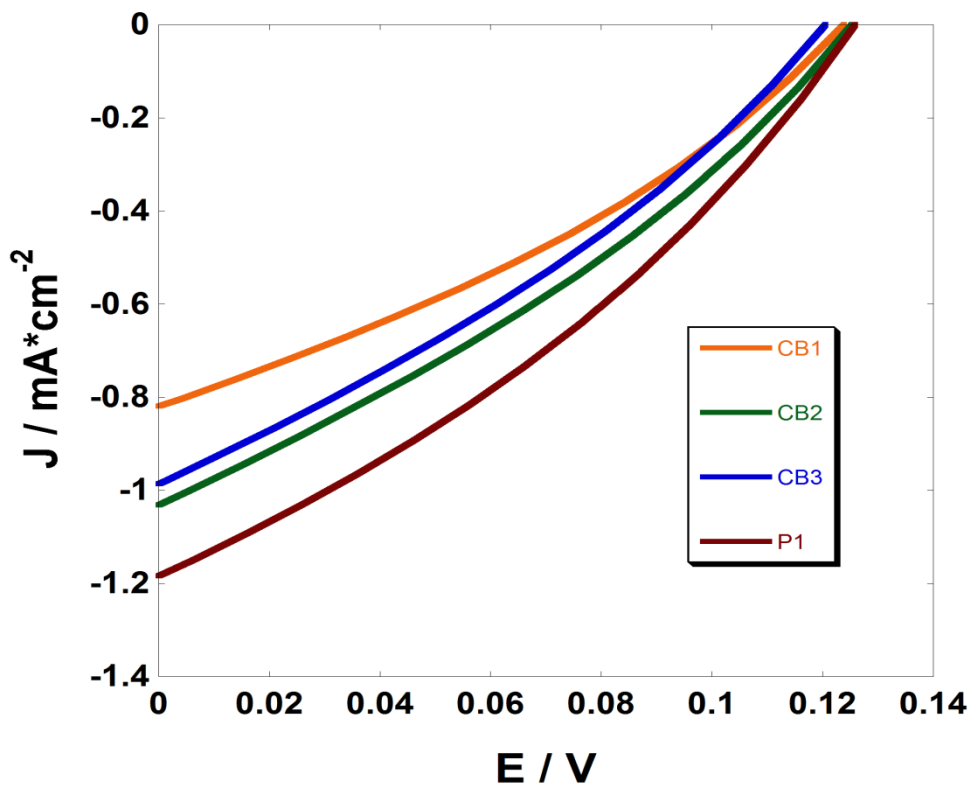


Figure 2. Transmittance spectra of NiO sensitized with four different dye compared with NiO/P1. Black line refers to the unsensitized electrode.

The electrical characterization of the fabricated devices has been performed under simulated solar radiation and the characteristic JV curves are shown in Figure 4. A reference cell sensitized with a high level benchmark as P1 dye[52] has been fabricated and tested as well: its electrical characterization is reported in Figure 4. From JV curves some key parameters as open circuit voltage (V_{OC} in mV), short circuit density (J_{SC} in $\text{mA}\cdot\text{cm}^{-2}$), fill factor (FF, %) and overall efficiency (η , %) could be obtained. The values of these parameters, averaged on five nominally equal devices have been reported in Table 2.

All the devices based on the reported dyes present interesting photoelectrochemical activity proving their efficiency as photosensitizers for p -DSSC. The best performing device is the one based on dye

193 **CB2** with a power conversion efficiency of 0.040 %. The devices based on dyes **CB1** and **CB3**
 194 afforded similar performances showing PCE values of 0.032 and 0.034 %, respectively. The
 195 obtained performances are only slightly lower that of the reference cell based on **P1** ($\eta = 0.049$ %).



196
 197 **Figure 3.** JV curves of NiO-based device sensitized with four different sensitizers and compared
 198 with a reference cell NiO/P1. The reported curves refer to the most performing device for each dye.

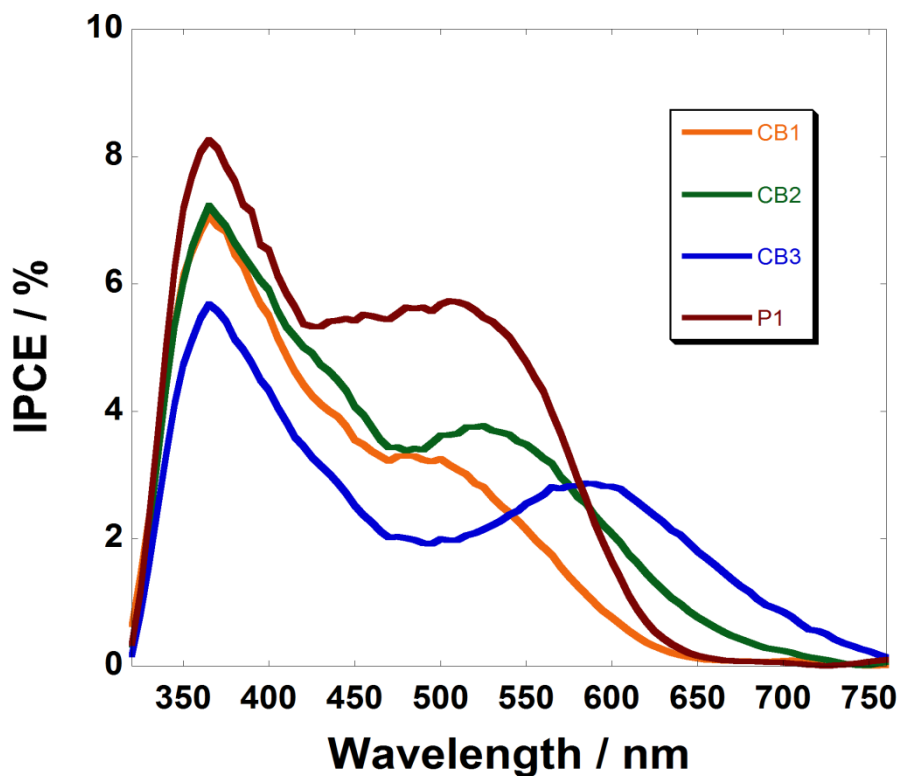
200 **Table 2.** Characteristic values of the parameters characterizing the photoelectrochemical
 201 performance of the *p*-DSSCs sensitized with the pyran based dyes of Figure 1 and P1 benchmark.

	$J_{sc} / \text{mA cm}^{-2}$	V_{oc} / mV	$FF / \%$	$\eta / \%$
CB1	-0.780 ± 0.017	124.3 ± 0.3	32.6 ± 0.5	0.032 ± 0.002
CB2	-1.000 ± 0.033	124.1 ± 0.4	32.3 ± 0.3	0.040 ± 0.002
CB3	-0.844 ± 0.027	122.7 ± 1.1	31.0 ± 0.6	0.034 ± 0.002
P1 (ref)	-1.188	125.6	32.9	0.049

202
 203 From the examination of the various electrical parameters reported in Table 2, it seems evident that
 204 V_{oc} values are not strongly dependent on the dye used to sensitize NiO. This is quite expected since
 205 all the dyes own similar molecular structures that differ just for the acceptor group (Figure 1).
 206 Nevertheless, this unit is quite far away from the NiO surface and it should hardly influence the

207 energetic modulation of the semiconductor valence band. The same explanation could be used to
1
208 justify the similarity in FF values. In fact, FF is deeply linked to open circuit potential value[53]. In
2
3
4
209 this case, the higher the latter the higher the former. The different overall efficiency values reported
5
6
210 in Table 2 are mainly controlled by the differences in the photocurrent produced by each device.
7
8
211 **CB2/NiO** device is the sole cell able to supply a current density higher than 1 mA/cm⁻². **CB1/NiO**
9
10
11 and **CB3/NiO** cells provide slightly lower current density that led to overall efficiency of 0.032 %
12
13
14 and 0.034 %, respectively. This behaviour is consistent with the different molar absorption
15
16
17 coefficients of the dyes: the higher is the latter, the higher is the efficiency of the cell. Therefore, we
18
19
20 could hypothesize that the here reported difference are mainly due to the light harvesting efficiency
21
22 (LHE) of each dye whereas the photo-injection efficiency is unvaried no matter of the sensitizer
23
24 employed.

25
26
27 The results obtained by *JV* curves have been strengthened by IPCE spectral measurements (Figure 5).
28



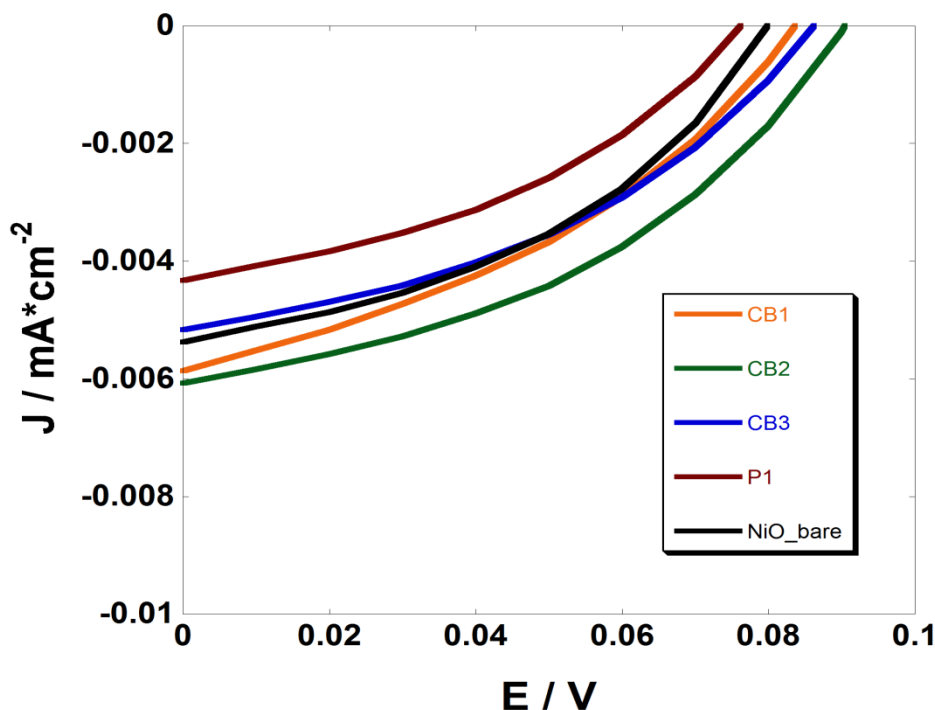
219
220 **Figure 4.** IPCE spectra of NiO-based devices sensitized with the different dyes and compared with
221 a reference cell NiO/P1. The reported spectra refer to the most performing device for each dye.
222

223
224
225
226
227
228
229
230
231
232
233
234
235
236
237
238
239
240
241
242
243
244
245
246
247
248
249
250
251
252
253
254
255
256
257
258
259
260
261
262
263
264
265

223 The IPCE profiles directly provides the percentage of incident photons that are converted into
1
224 electrons for each wavelength of the incident radiation. In our case, the peak at shorter wavelengths
2
3
4
225 ($\lambda < 420$ nm) is due to the intrinsic photoactivity of NiO (especially Ni³⁺ available sites)[48,54]
5
6
226 whereas the broad peak at longer wavelength is characteristic of each sensitizer. IPCE spectra give
7
8
227 us some additional information with respect to *JV* curves. Interestingly, the intensity of the IPCE
9
10
11
228 peak characteristic of NiO decreases with the increase of the steric hindrance of the acceptor group.
12
13
229 At this regard we expect that the bulkiness of the EWG might influence the extent of dye-loading
14
15
16
230 with the larger groups preventing the anchoring of dye-sensitizers at large surface concentrations
17
18
231 with respect to the colorants with relatively smaller size. Nevertheless, the goodness of each device
19
20
21
232 performances is mainly linked to the dye peak. Better efficiencies have been recorded when the
22
23
24
233 sensitizer IPCE peak is high and/or broad.
25

26
234 It is well know that non stoichiometric NiO promotes triiodide reduction even in dark
27
28
235 conditions[54]. In order to prove the magnitude of the dark reduction of triiodide to iodide ($I_3^- + 2e^-$
29
30
31
236 $\rightarrow 3 I^-$) dark *JV* curves measurements (Figure 6) were conducted on the most performing devices.
32
33
34
237 The dark reduction process occurs at both NiO/electrolyte and at the FTO/electrolyte interfaces. The
35
36
238 FTO can participate in the electrochemical process if some channels are present through the porous
37
38
39
239 film of NiO semiconductor. This morphological characteristic allows the penetration of the
40
41
240 electrolyte till the substrate of charge collection. In our case, we are not going to consider the
42
43
44
241 charge transfer process at the FTO/electrolyte interface. In dark conditions, the *p*-DSSC devices
45
46
242 here characterized feature a higher open circuit voltage as compared to devices based on
47
48
243 unsensitized NiO cathode. Therefore, we could state that a part of the NiO/dye surface charge arise
49
50
51
244 either from a dark charge transfer process between the sensitizer and the semiconductor film or
52
53
245 from the spontaneous adsorption of some anion[55,56]. The extent of the latter phenomenon
54
55
56
246 depends on the surface concentration of the sensitizer, its anchoring geometry and the nature of the
57
58
247 adsorbed anion.
59
60
61
62
63
64
65

248 Some further information could be obtained by the analyses of dark J_{SC} on the nature of the dye
 1
 249 (Table 3). The sensitization of NiO electrodes with **CCB2** and **CB1** produces cell with a larger
 3
 4
 250 value of dark current density with respect to bare NiO cathode.
 5
 6



251
 252 **Figure 5.** In dark JV curves of NiO-based device sensitized with three different sensitizers and
 253 compared with a reference cell NiO/P1 and bare NiO devices. The reported curves refer to the most
 254 performing device for each dye.
 255
 256

257 **Table 3.** Characteristic values of *p*-DSSC parameters obtained from the JV curves recorded in dark
 258 conditions

	CB1	CB2	CB3	P1	NiO bare
V_{oc} / mV	83	90	86	76	80
$J_{sc} / \mu\text{A cm}^{-2}$	5.9	6.1	5.2	4.3	5.3

259 This evidence implicates that these two dyes mediate the dark process of electron transfer from the
 260 semiconductor to triiodide anion. Conversely, **CB3**/NiO device showed a dark current very close to
 261 that of the bare NiO device while **P1**/NiO cell afforded a reduced dark current indicating that **P1**
 262 behaves actually as an agent of passivation towards the dark reduction process, as already reported
 263
 264
 265

263 by a previous work realized with different electrodes of mesoporous NiO[54]. Nevertheless, it is
1
264 mandatory to remark that the dark currents constitute less than 2% of the photocurrent.
3

4
265

266 CONCLUSIONS

267
268

268 Three custom-made full organic dyes have been employed to sensitize screen-printed NiO
11
12
269 photocathodes for *p*-DSSC. The dyes are based on a pyran core that has been functionalized with
13
14
270 different electron acceptor groups and symmetrically coupled to two phenothiazine donor moieties.
16

17
271 The latter moieties bear carboxylic groups which act as anchoring units. Such a design is based on
18
19
272 the placement of the electron acceptor group in a site far away from the anchoring carboxylic
21
22
273 groups that bind to the NiO surface. Such a structural feature is highly desirable to reduce the
23
24
274 internal recombination between the LUMO of the dye and the VB of NiO with resulting
26
275 enhancement of the cell performances. The optical properties of the sensitizers in solution and in the
28
29
276 NiO immobilized state have been evaluated before their employment in a complete device. All dyes
30
31
277 experimented a very good binding onto the electrode surface as evidenced by transmittance spectra.
33

34
278 When implemented in a complete device, dye **CB2** showed the best photoelectrochemical
35
36
279 performance by displaying a photocurrent density of short circuit larger than 1 mA cm⁻² and an
38
39
280 overall efficiency of 0.04%. These results are just slightly lower than the values reported for a high
40
41
281 performing reference cell like the *p*-DSSC employing P1 as benchmark sensitizer. The comparison
43
44
282 of the IPCE spectra evidence that dye **CB2** gives the higher efficiency thanks to a more efficient
45
46
283 light harvesting efficiency due to its higher molar extinction coefficient with respect to the other
48
49
284 sensitizers.

50
51
285 In conclusion, the sensitizers here proposed have showed a very good photoelectrochemical
52
53
286 behavior in *p*-DSSCs when screen-printed NiO is the cathode. In future works some similar dyes
55
56
287 will be investigated to optimize the molecular skeleton as well as the nature and strength of the
57
58
288 electron withdrawing group. The optimization will be conducted in the perspective of applying
60
61
289 these dyes as sensitizers of *p*-DSSC device.
62
63
64
65

290
1
291
2
3
292
293
6
294
295
9
10
296
11
297
12
298
13
14
299
1300
17
1301
1302
20
1303
21
22
1304
23
24
1305
25
1306
26
1307
28
1308
29
1309
30
31
1310
32
1311
33
34
1312
35
1313
36
37
1314
38
1315
40
1316
41
42
1317
43
1318
44
1319
45
46
1320
48
1321
49
50
1322
51
1323
52
1324
53
54
1325
55
1326
56
57
1327
58
1328
60
1329
61
62
63
64
65

REFERENCES

- [1] A. Hagfeldt, G. Boschloo, L. Sun, L. Kloo, H. Pettersson, Dye-Sensitized Solar Cells, *Chem. Rev.* 110 (2010) 6595. doi:10.1021/cr900356p.
- [2] C. Cavallo, F. Di Pascasio, A. Latini, M. Bonomo, D. Dini, Nanostructured Semiconductor Materials for Dye-Sensitized Solar Cells, *J. Nanomater.* 2017 (2017) 5323164.
- [3] M. Ye, X. Wen, M. Wang, J. Iocozzia, N. Zhang, C. Lin, et al., Recent advances in dye-sensitized solar cells: From photoanodes, sensitizers and electrolytes to counter electrodes, *Mater. Today.* 18 (2015) 155–162. doi:10.1016/j.mattod.2014.09.001.
- [4] M.K. Nazeeruddin, E. Baranoff, M. Grätzel, Dye-sensitized solar cells: A brief overview, *Sol. Energy.* 85 (2011) 1172–1178. doi:10.1016/j.solener.2011.01.018.
- [5] A. Mishra, M.K.R. Fischer, P. Büuerle, Metal-Free organic dyes for dye-Sensitized solar cells: From structure: Property relationships to design rules, *Angew. Chemie - Int. Ed.* 48 (2009) 2474–2499. doi:10.1002/anie.200804709.
- [6] J. Gong, J. Liang, K. Sumathy, Review on dye-sensitized solar cells (DSSCs): Fundamental concepts and novel materials, *Renew. Sustain. Energy Rev.* 16 (2012) 5848–5860. doi:10.1016/j.rser.2012.04.044.
- [7] P. Docampo, S. Guldin, T. Leijtens, N.K. Noel, U. Steiner, H.J. Snaith, Lessons learned: From dye-sensitized solar cells to all-solid-state hybrid devices, *Adv. Mater.* 26 (2014) 4013–4030. doi:10.1002/adma.201400486.
- [8] Z. Ning, Y. Fu, H. Tian, Improvement of dye-sensitized solar cells: What we know and what we need to know, *Energy Environ. Sci.* 3 (2010) 1170–1181. doi:10.1039/c003841e.
- [9] M.A. Green, S.P. Bremner, Energy Conversion Approaches and Materials for High Efficiency Photovoltaics, *Nat. Mater.* 16 (2017) 23–34. doi:10.1038/nmat4676.
- [10] S. Yoon, S. Tak, J. Kim, Y. Jun, K. Kang, J. Park, Application of transparent dye-sensitized solar cells to building integrated photovoltaic systems, *Build. Environ.* 46 (2011) 1899–1904. doi:10.1016/j.buildenv.2011.03.010.
- [11] A. Fakharuddin, R. Jose, T.M. Brown, F. Fabregat-Santiago, J. Bisquert, A perspective on the production of dye-sensitized solar modules, *Energy Environ. Sci.* 7 (2014) 3952–3981. doi:10.1039/c4ee01724b.
- [12] B. O'Regan, M. Gratzel, A low-cost, high-efficiency solar cell based on dye-sensitized colloidal TiO₂ films, *Nature.* 353 (1991) 737.
- [13] K. Kakiage, Y. Aoyama, T. Yano, K. Oya, J. Fujisawa, M. Hanaya, Highly-efficient dye-sensitized solar cells with collaborative sensitization by silyl-anchor and carboxy-anchor dyes, *Chem. Commun.* 51 (2015) 15894–15897. doi:10.1039/C5CC06759F.
- [14] M. Bonomo, D. Dini, Nanostructured p-type semiconductor electrodes and photoelectrochemistry of their reduction processes, *Energies.* 9 (2016). doi:10.3390/en9050373.
- [15] C.J. Wood, G.H. Summers, E.A. Gibson, Increased photocurrent in a tandem dye-sensitized solar cell by modifications in push–pull dye-design, *Chem. Commun.* 51 (2015) 3915. doi:10.1039/c4cc10230d.

- 330 [16] F. Odobel, Y. Pellegrin, E.A. Gibson, A. Hagfeldt, A.L. Smeigh, L. Hammarström, Recent advances and
331 future directions to optimize the performances of p-type dye-sensitized solar cells, *Coord. Chem.*
332 *Rev.* 256 (2012) 2414–2423. doi:http://dx.doi.org/10.1016/j.ccr.2012.04.017.
3
- 333 [17] F. Odobel, L. Le Pleux, Y. Pellegrin, E. Blart, New photovoltaic devices based on the sensitization of p-
334 type semiconductors: Challenges and opportunities, *Acc. Chem. Res.* 43 (2010) 1063–1071.
335 doi:10.1021/ar900275b.
- 336 [18] N. Li, E.A. Gibson, P. Qin, G. Boschloo, M. Gorlov, A. Hagfeldt, et al., Double-layered NiO
337 photocathodes for p-Type DSSCs with record IPCE, *Adv. Mater.* 22 (2010) 1759–1762.
338 doi:10.1002/adma.200903151.
- 339 [19] F. Odobel, Y. Pellegrin, Recent advances in the sensitization of wide-band-gap nanostructured p-type
340 semiconductors. photovoltaic and photocatalytic applications, *J. Phys. Chem. Lett.* 4 (2013) 2551–
341 2564. doi:10.1021/jz400861v.
- 342 [20] A. Nattestad, A.J. Mozer, M.K.R. Fischer, Y.-B. Cheng, A. Mishra, P. Bauerle, et al., Highly efficient
343 photocathodes for dye-sensitized tandem solar cells, *Nat Mater.* 9 (2010) 31.
- 344 [21] D. Xiong, W. Chen, Recent progress on tandem structured dye-sensitized solar cells, *Front.*
345 *Optoelectron.* 5 (2012) 371–389. doi:10.1007/s12200-012-0283-9.
- 346 [22] W. Shockley, H.J. Queisser, Detailed balance limit of efficiency of p-n junction solar cells, *J. Appl.*
347 *Phys.* 32 (1961) 510. doi:10.1063/1.1736034.
- 348 [23] Y. Xu, T. Gong, J.N. Munday, The generalized Shockley-Queisser limit for nanostructured solar cells,
349 *Sci. Rep.* 5 (2015) 13536. doi:10.1038/srep13536.
- 350 [24] I. Sullivan, B. Zoellner, P.A. Maggard, Copper(I)-Based p-Type Oxides for Photoelectrochemical and
351 Photovoltaic Solar Energy Conversion, *Chem. Mater.* 28 (2016) 5999.
352 doi:10.1021/acs.chemmater.6b00926.
- 353 [25] I.R. Perera, T. Daeneke, S. Makuta, Z. Yu, Y. Tachibana, A. Mishra, et al., Application of the
354 tris(acetylacetonato)iron(III)/(II) redox couple in p-type dye-sensitized solar cells, *Angew. Chemie -*
355 *Int. Ed.* 54 (2015) 3758. doi:10.1002/anie.201409877.
- 356 [26] L. D'Amario, L.J. Antila, B. Pettersson Rimgard, G. Boschloo, L. Hammarström, Kinetic evidence of
357 two pathways for charge recombination in NiO-based dye-sensitized solar cells, *J. Phys. Chem. Lett.*
358 6 (2015) 779–783. doi:10.1021/acs.jpcclett.5b00048.
- 359 [27] T. Jiang, M. Bujoli-Doeuff, Y. Farré, Y. Pellegrin, E. Gautron, M. Boujtita, et al., CuO nanomaterials for
360 p-type dye-sensitized solar cells, *RSC Adv.* 6 (2016) 112765. doi:10.1039/C6RA17879K.
- 361 [28] X. Li, F. Yu, S. Stappert, C. Li, Y. Zhou, Y. Yu, et al., Enhanced Photocurrent Density by Spin-Coated
362 NiO Photocathodes for N-Annulated Perylene-Based p-Type Dye-Sensitized Solar Cells, *ACS Appl.*
363 *Mater. Interfaces.* 8 (2016) 19393. doi:10.1021/acsami.6b04007.
- 364 [29] T.T.T. Pham, S.K. Saha, D. Provost, Y. Farré, M. Raissi, Y. Pellegrin, et al., Toward Efficient Solid-State
365 p-Type Dye-Sensitized Solar Cells: The Dye Matters, *J. Phys. Chem. C.* 121 (2017) 129–139.
366 doi:10.1021/acs.jpcc.6b10513.
- 367 [30] Y. Farré, L. Zhang, Y. Pellegrin, A. Planchat, E. Blart, M. Boujtita, et al., Second Generation of
368 Diketopyrrolopyrrole Dyes for NiO-Based Dye-Sensitized Solar Cells, *J. Phys. Chem. C.* 120 (2016)
369 7923–7940. doi:10.1021/acs.jpcc.5b12489.
- 370 [31] J. Cui, J. Lu, X. Xu, K. Cao, Z. Wang, G. Alemu, et al., Organic sensitizers with pyridine ring anchoring
371 group for p-type dye-sensitized solar cells, *J. Phys. Chem. C.* 118 (2014) 16433–16440.
- 372
373
374
375

- 372 doi:10.1021/jp410829c.
- 1
373 [32] Z. Liu, W. Li, S. Topa, X. Xu, X. Zeng, Z. Zhao, et al., Fine tuning of fluorene-based dye structures for
374 high-efficiency p -type dye-sensitized solar cells, *ACS Appl. Mater. Interfaces*. 6 (2014) 10614–10622.
375 doi:10.1021/am5022396.
- 5
376 [33] B.B. Jung, C. Yoon, H. Shim, L. Do, T. Zyung, Pure-Red Dye for Organic Electroluminescent Devices :
377 Bis-Condensed DCM Derivatives **, *Adv. Funtional Mater.* 11 (2001) 430–434. doi:10.1002/1616-
378 3028(200112)11:6<430::AID-ADFM430>3.0.CO;2-G.
- 10
379 [34] L. Yang, M. Guan, D. Nie, B. Lou, Z. Liu, Z. Bian, et al., Efficient, saturated red electroluminescent
380 devices with modified pyran-containing emitters, *Opt. Mater. (Amst)*. 29 (2007) 1672–1679.
381 doi:10.1016/j.optmat.2006.09.013.
- 14
382 [35] L. Xue, J. He, X. Gu, Z. Yang, B. Xu, W. Tian, Efficient bulk-heterojunction solar cells based on a
383 symmetrical D-π-A-D organic dye molecule, *J. Phys. Chem. C*. 113 (2009) 12911–12917.
384 doi:10.1021/jp902976w.
- 19
385 [36] Z. Li, Q. Dong, S. Yao, J. Qian, Y. Wang, F. Jiang, et al., An efficient photovoltaic device based on
386 novel D-π-A-D solution-processable small molecules, *J. Mater. Sci.* 50 (2014) 937–947.
387 doi:10.1007/s10853-014-8653-x.
- 23
388 [37] A. Carella, F. Borbone, U. Caruso, R. Centore, A. Roviello, A. Barsella, et al., NLO behavior of
389 polymers containing Y-shaped chromophores, *Macromol. Chem. Phys.* 208 (2007) 1900–1907.
390 doi:10.1002/macp.200700275.
- 27
391 [38] P. Shao, Z. Huang, J. Li, S. Chen, J. Luo, J. Qin, et al., Two-photon absorption properties of two
392 (dicyanomethylene)-pyran derivatives, *Opt. Mater. (Amst)*. 29 (2006) 337–341.
393 doi:10.1016/j.optmat.2005.08.039.
- 32
394 [39] A. Ambrosio, P. Maddalena, A. Carella, F. Borbone, A. Roviello, M. Polo, et al., Two-photon induced
395 self-structuring of polymeric films based on Y-shape azobenzene chromophore, *J. Phys. Chem. C*.
396 115 (2011) 13566–13570. doi:10.1021/jp200050h.
- 36
397 [40] D. Dini, M.J.F. Calvete, M. Hanack, Nonlinear Optical Materials for the Smart Filtering of Optical
398 Radiation, *Chem. Rev.* 116 (2016) 13043–13233. doi:10.1021/acs.chemrev.6b00033.
- 39
400 [41] A. Ambrosio, E. Orabona, P. Maddalena, A. Camposeo, M. Polo, A.A.R. Neves, et al., Two-photon
401 patterning of a polymer containing Y-shaped azochromophores, *Appl. Phys. Lett.* 94 (2009) 11115.
402 doi:10.1063/1.3058820.
- 44
403 [42] Y. Liu, Y. Liu, D. Zhang, H. Hu, C. Liu, Theoretical investigation on second-order nonlinear optical
404 properties of (dicyanomethylene) -pyran derivatives, *J. Mol. Struct.* 570 (2001) 43–51.
405 doi:10.1016/S0022-2860(01)00479-3.
- 48
406 [43] S. Franco, J. Garín, N. Martínez De Baroja, R. Pérez-Tejada, J. Orduna, Y. Yu, et al., New D-π-A-
407 conjugated organic sensitizers based on 4 H-pyran-4-ylidene donors for highly efficient dye-
408 sensitized solar cells, *Org. Lett.* 14 (2012) 752–755. doi:10.1021/ol203298r.
- 53
409 [44] C. Maglione, A. Carella, R. Centore, S. Fusco, A. Velardo, A. Peluso, et al., Tuning optical absorption
410 in pyran derivatives for DSSC, *J. Photochem. Photobiol. A Chem.* 321 (2016) 79–89.
411 doi:10.1016/j.jphotochem.2016.01.018.
- 57
412 [45] C. Maglione, A. Carella, C. Carbonara, R. Centore, S. Fusco, A. Velardo, et al., Novel pyran based dyes
413 for application in dye sensitized solar cells, *Dye. Pigment.* 133 (2016) 395–405.
414 doi:10.1016/j.dyepig.2016.06.024.
- 62
63
64
65

- 414 [46] M. Bonomo, N. Barbero, F. Matteocci, A. Di Carlo, C. Barolo, D. Dini, Beneficial Effect of Electron-
415 Withdrawing Groups on the Sensitizing Action of Squaraines for p-Type Dye-Sensitized Solar Cells, *J.*
416 *Phys. Chem. C.* 120 (2016) 16340–16353. doi:10.1021/acs.jpcc.6b03965.
3
- 417 [47] G. Boschloo, A. Hagfeldt, Characteristics of the iodide/triiodide redox mediator in dye-sensitized
418 solar cells, *Acc. Chem. Res.* 42 (2009) 1819–1826. doi:10.1021/ar900138m.
419
- 419 [48] M. Bonomo, G. Naponiello, I. Venditti, V. Zardetto, A. Di Carlo, D. Dini, Electrochemical and
420 Photoelectrochemical Properties of Screen-Printed Nickel Oxide Thin Films Obtained from Precursor
421 Pastes with Different Compositions, *J. Electrochem. Soc.* 164 (2017) H137–H147.
422 doi:10.1149/2.0051704jes.
12
- 423 [49] F. De Rossi, L. Di Gaspare, A. Reale, A. Di Carlo, T.M. Brown, Blending CoS and Pt for amelioration of
424 electrodeposited transparent counterelectrodes and the efficiency of back-illuminated dye solar
425 cells, *J. Mater. Chem. A.* 1 (2013) 12941. doi:10.1039/c3ta13076b.
14
15
16
- 426 [50] J. He, H. Lindström, A. Hagfeldt, S.-E. Lindquist, Dye-Sensitized Nanostructured p-Type Nickel Oxide
427 Film as a Photocathode for a Solar Cell, *J. Phys. Chem. B.* 103 (1999) 8940. doi:10.1021/jp991681r.
17
18
19
- 428 [51] G. Natu, P. Hasin, Z. Huang, Z. Ji, M. He, Y. Wu, Valence band-edge engineering of nickel oxide
429 nanoparticles via cobalt doping for application in p-type dye-sensitized solar cells, *ACS Appl. Mater.*
430 *Interfaces.* 4 (2012) 5922–5929. doi:10.1021/am301565j.
20
21
22
23
24
- 431 [52] P. Qin, H. Zhu, T. Edvinsson, G. Boschloo, A. Hagfeldt, L. Sun, Design of an Organic Chromophore for
432 P-Type Dye-Sensitized Solar Cells, *J. Am. Chem. Soc.* 130 (2008) 8570. doi:10.1021/ja8001474.
25
26
27
- 433 [53] T. Daeneke, Z. Yu, G.P. Lee, D. Fu, N.W. Duffy, S. Makuta, et al., Dominating energy losses in NiO p-
434 type dye-sensitized solar cells, *Adv. Energy Mater.* 5 (2015) 1401387. doi:10.1002/aenm.201401387.
28
29
30
- 435 [54] S. Sheehan, G. Naponiello, F. Odobel, D.P. Dowling, A. Di Carlo, D. Dini, Comparison of the
436 photoelectrochemical properties of RDS NiO thin films for p-type DSCs with different organic and
437 organometallic dye-sensitizers and evidence of a direct correlation between cell efficiency and
438 charge recombination, *J. Solid State Electrochem.* 19 (2015) 975–986. doi:10.1007/s10008-014-
439 2703-9.
31
32
33
34
35
36
37
- 440 [55] M. Bonomo, A.G. Marrani, V. Novelli, M. Awais, D.P. Dowling, J.G. Vos, et al., Surface properties of
441 nanostructured NiO undergoing electrochemical oxidation in 3-methoxy-propionitrile, *Appl. Surf.*
442 *Sci.* 403 (2017) 441–447. doi:10.1016/j.apsusc.2017.01.202.
38
39
40
41
42
- 443 [56] M. Bonomo, D. Dini, A.G. Marrani, Adsorption Behavior of I³⁻ and I⁻ Ions at a Nanoporous
444 NiO/Acetonitrile Interface Studied by X-ray Photoelectron Spectroscopy, *Langmuir.* 32 (2016)
445 11540–11550. doi:10.1021/acs.langmuir.6b03695.
43
44
45
46
47
48

446

48

49

50

51

52

53

54

55

56

57

58

59

60

61

62

63

64

65

Table 1. Optical and electrochemical properties of the synthesized chromophores

Dye	λ_{\max} /nm ^a	ϵ /L·mol ⁻¹ ·cm ⁻¹ ^a	HOMO /eV ^b	LUMO / eV ^b
CB1	464	4.1·10 ⁴	-5.51	-3.51
CB2	521	4.3·10 ⁴	-5.51	-3.69
CB3	582	3.8·10 ⁴	-5.59	-3.95

a) Scan rate 200 nm/min, in THF solution; b) determined, as reported in ref. 38, by a combined electrochemical and optical approach on thin film of the dyes,.

Table 2. Characteristic values of the parameters characterizing the photoelectrochemical performance of the p-DSSCs sensitized with the pyran based dyes of Figure 1 and P1 benchmark.

	J_{sc} / mA cm ⁻²	V_{oc} /mV	FF / %	η / %
CB1	-0.780 ± 0.017	124.3 ± 0.3	32.6 ± 0.5	0.032 ± 0.002
CB2	-1.000 ± 0.033	124.1 ± 0.4	32.3 ± 0.3	0.040 ± 0.002
CB3	-0.844 ± 0.027	122.7 ± 1.1	31.0 ± 0.6	0.034 ± 0.002
P1 (ref)	-1.188	125.6	32.9	0.049

Table 3. Characteristic values of p-DSSC parameters obtained from the JV curves recorded in dark conditions

	CB1	CB2	CB3	P1	NiO bare
V_{oc} / mV	83	90	86	76	80
J_{sc} / μ A cm ⁻²	5.9	6.1	5.2	4.3	5.3

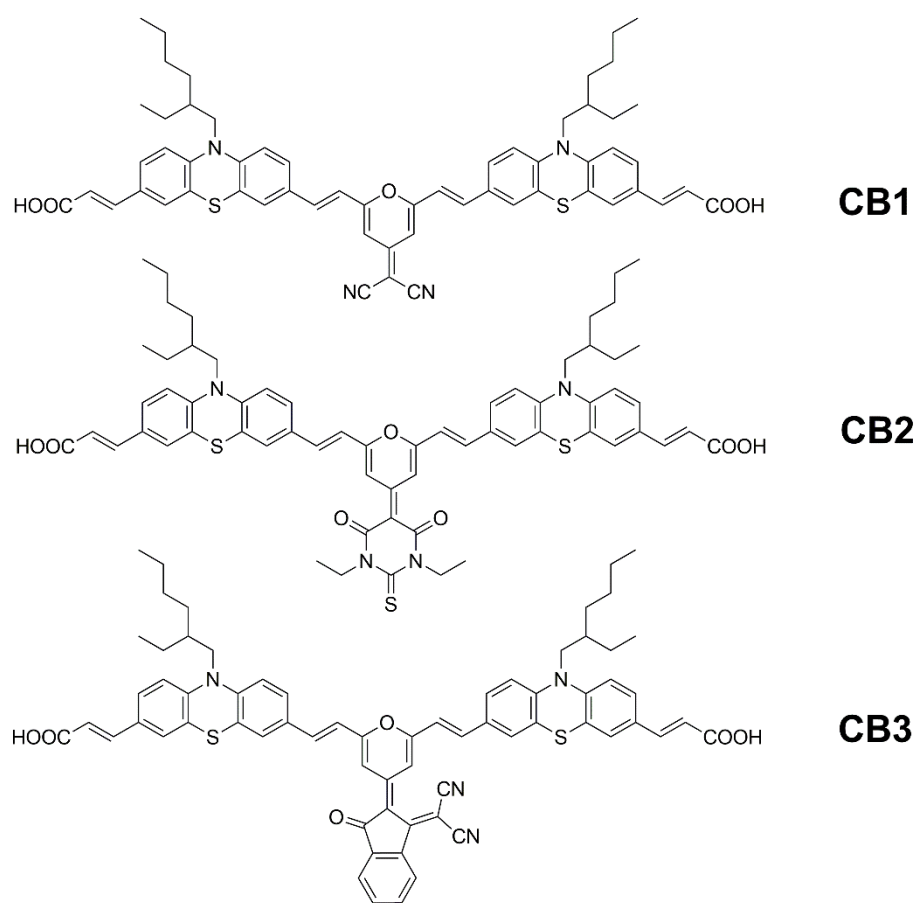


Figure 1. Chemical structures of the reported pyran based photosensitizers

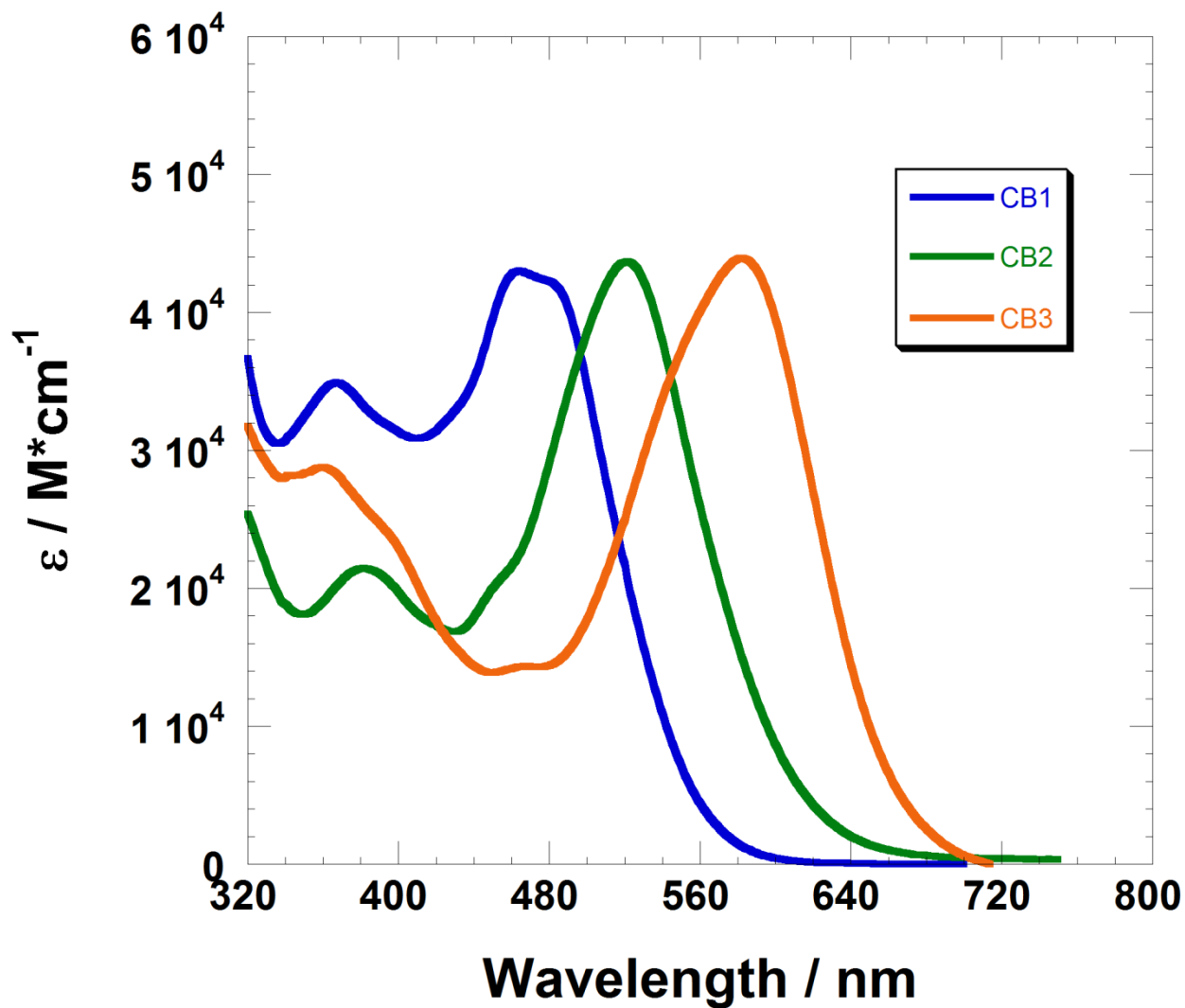


Figure 1. Molar absorptivity of the reported dyes in THF solution

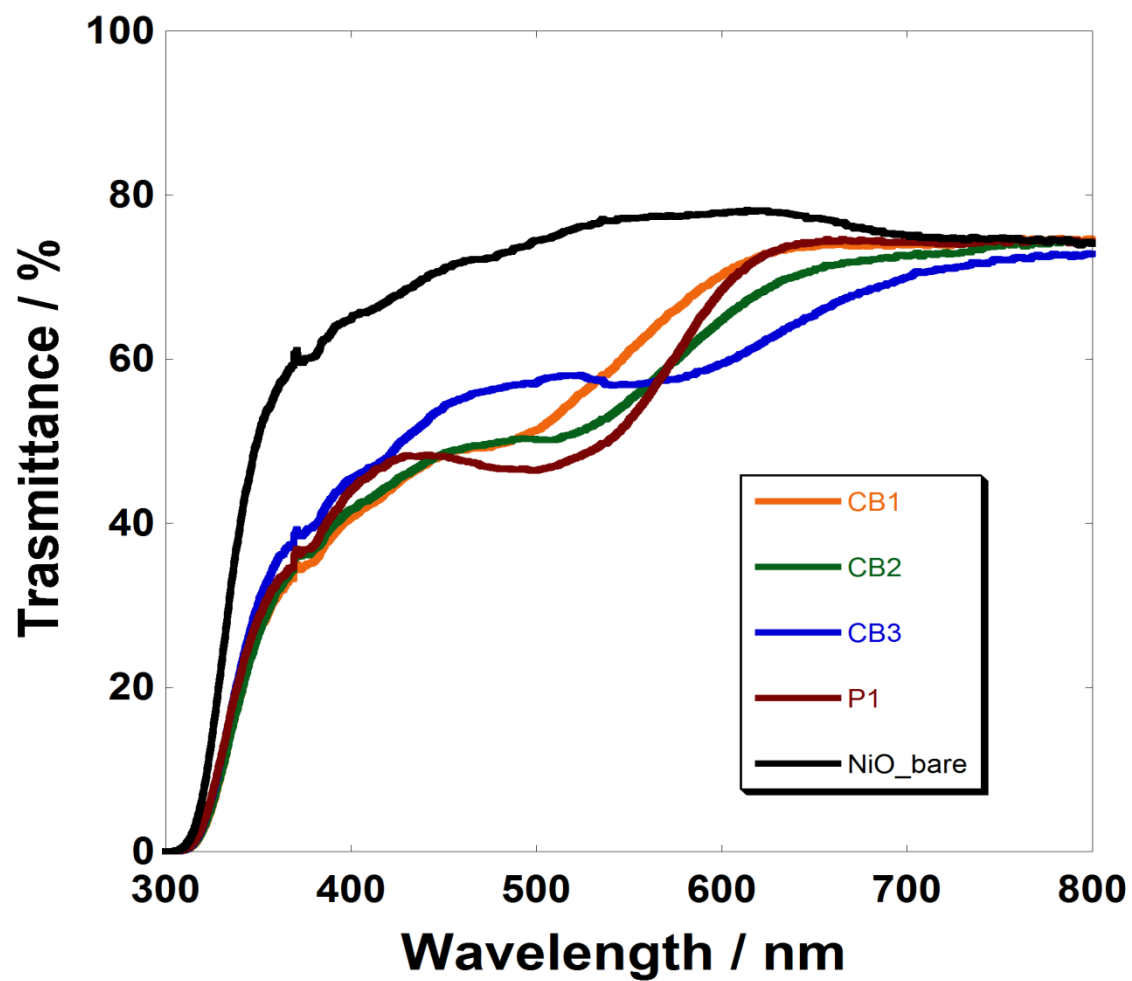


Figure 2. Transmittance spectra of NiO sensitized with four different dye compared with NiO/P1. Black line refers to the unsensitized electrode.

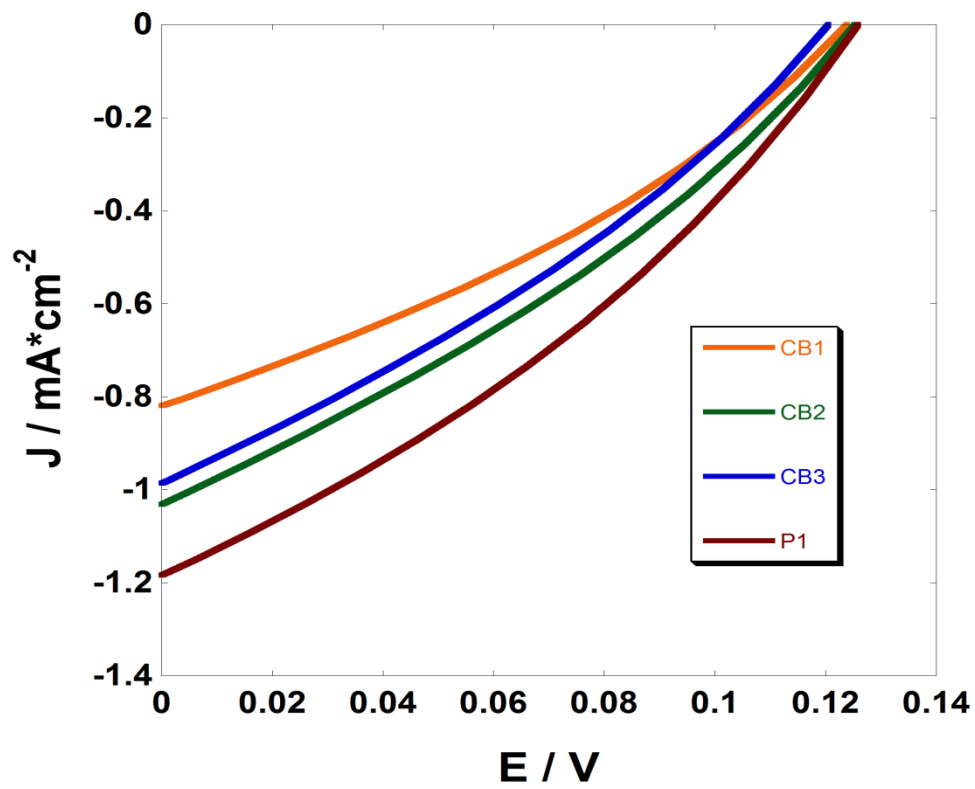


Figure 3. JV curves of NiO-based device sensitized with four different sensitizers and compared with a reference cell NiO/P1. The reported curves refer to the most performing device for each dye.

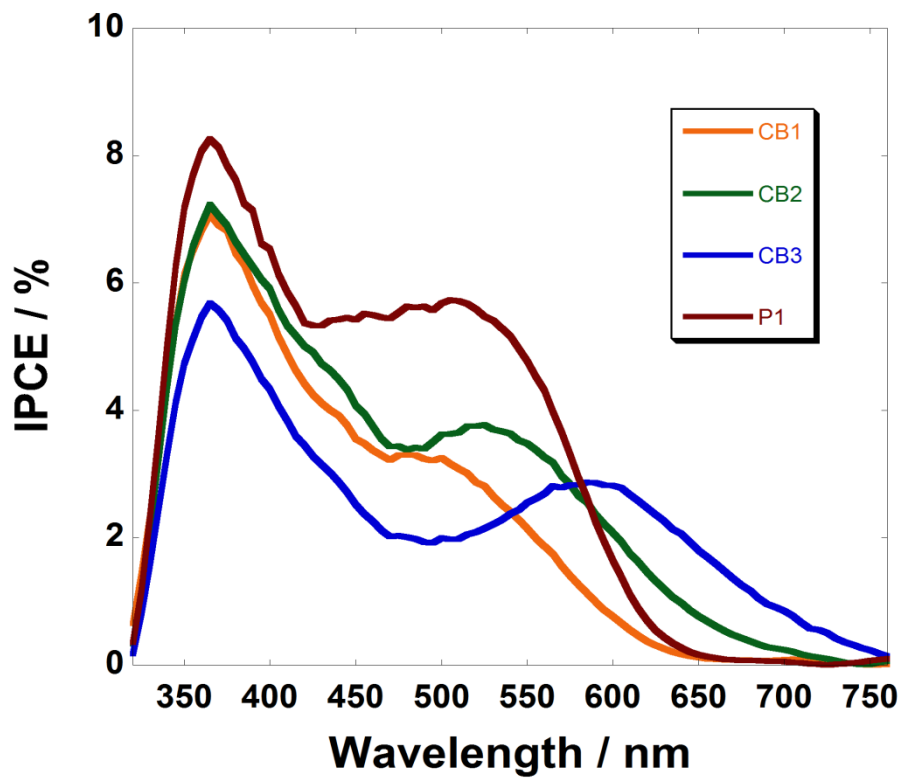


Figure 4. IPCE spectra of NiO-based devices sensitized with the different dyes and compared with a reference cell NiO/P1. The reported spectra refer to the most performing device for each dye.

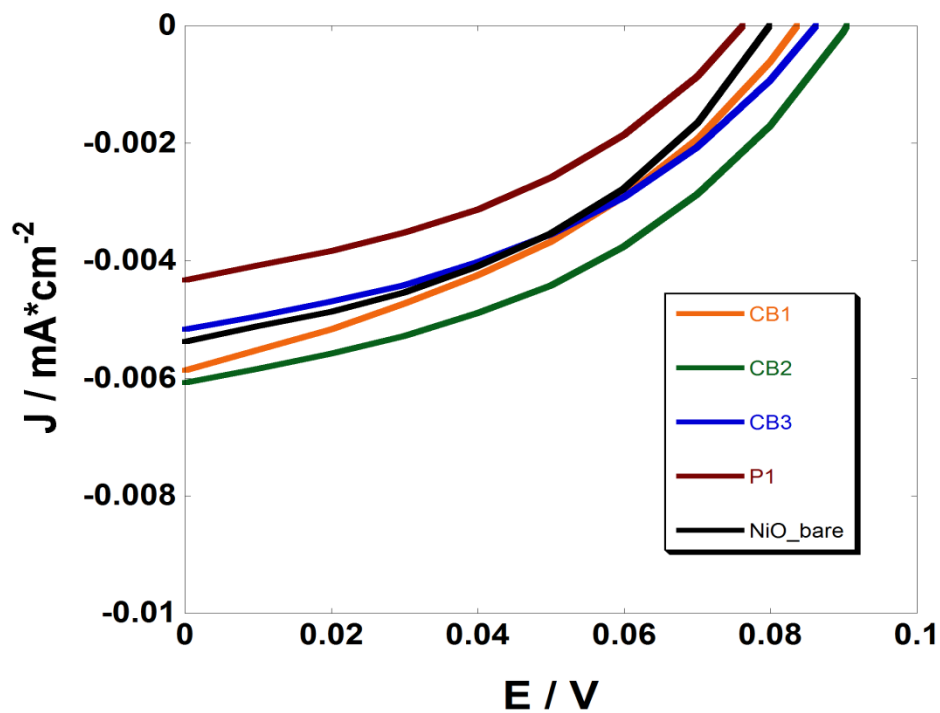


Figure 5. In dark JV curves of NiO-based device sensitized with three different sensitizers and compared with a reference cell NiO/P1 and bare NiO devices. The reported curves refer to the most performing device for each dye.

Highlights (for review)

- Electroactive NiO films are deposited via screen printing with NiO nanoparticles
- Screen-printed NiO is mesoporous
- New Pyran-based dyes has been tested as sensitizers in p-DSSC
- CV measurements reveals a good photoelectrochemical behavior for all the devices
- Overall efficiencies are comparable with P1-based device